RSC Advances

RSC Publishing

PAPER

View Article Online
View Journal | View Issue



Cite this: *RSC Advances*, 2013, **3**, 5845

# *In situ* monitoring of electrophoretic deposition of $Cu_2ZnSnS_4$ nanocrystals†

Kai Kornhuber,[a] Jaison Kavalakkatt,[a] Xianzhong Lin,[a] Ahmed Ennaoui*[a] and Martha Ch. Lux-Steiner[ab]

Received 28th November 2012,
Accepted 31st January 2013

DOI: 10.1039/c3ra23093g

**www.rsc.org/advances**

$Cu_2ZnSnS_4$ (CZTS) nanocrystal (NC) layers were deposited successfully by electrophoretic deposition (EPD) on molybdenum and fluorine doped tin oxide coated glass substrates. This approach combines a non-vacuum coating technique known for its industrial eligibility to a solar absorber material consisting solely of non-toxic and earth abundant elements. CZTS NC layers with thicknesses between 200 nm and 1.5 μm were formed in 0.5 to 1 min while the NC dispersion, consisting of organic solvents, depleted entirely. Therefore the layer thickness can be controlled by varying the concentration of NCs in dispersion. Scanning electron microscopy micrographs show compact and homogeneous films. The layers were analyzed by grazing incidence X-ray diffraction, Raman analysis. Optical properties were probed by UV-vis spectroscopy. The dependence of dispersion composition and applied voltage on deposition dynamics and duration was analyzed by the use of an optical monitoring setup. The results open up a route of low cost CZTS thin film fabrication with reduced chemical contamination, fast layer deposition and high raw material use.

## Introduction

In this work, a route to deposit $Cu_2ZnSnS_4$ (CZTS) nanocrystals (NCs) by electrophoretic deposition (EPD) is introduced. Electrophoretic deposition (EPD) is a two-step process, combining the movement of charged particles in suspension under the influence of a static-electrical field (electrophoresis) and their subsequent deposition on one or both of the field generating electrodes. Due to the relatively simple setup (basically a power supply) without the requirement of high vacuum, EPD is considered a low cost deposition technique. Especially in the tile and sanitary industry the high deposition speed and the possibility of automation are being valued.[1,2] It has been shown, that due to its high throw power, objects of complex shapes can be covered, up to infiltration of porous materials or woven fiber preforms. Electrophoretic processes are widely used in the automotive industry to cover car parts with protective layers.[2] Additional qualities connected to the EPD process are low material losses, improved adherence, high density of films, potential reuse of not deposited material in suspension and the possibility of large area coatings. EPD of nanostructures of single elements and compound material has been achieved.[3] Nanomaterials of different shapes have been deposited *via* EPD, among them nanorods and nanotubes.[4–6]

In order to show EPD-activity the dispersed particles require a non-zero surface charge. EPD has been shown from organic and aqueous solvents. A good overview on the processes that lead to charge generation and dispersion stability is provided in the review of Sarkar and Nicholson.[1]

CZTS is a quaternary p-type semiconductor with optimal optoelectronic properties ($E_g$ = 1.5 eV, absorption coefficient $\sim 10^4$ $cm^{-1}$) to serve as absorber material for thin film solar cells.[7–9] Its constituents are non-toxic and earth abundant. Therefore CZTS is considered as an attractive alternative to established thin film solar cell materials. In analogy to the $Cu(In,Ga)(S,Se)_2$ system the band gap can be tuned by the integration of Se atoms, leading to energy conversion efficiencies of 11.1% in a hydrazine solution based process.[10] Hydrazine, however, is very toxic and explosive and must be handled with great care. Efficiencies of 8.4% and 6.8% have been accomplished by thermal evaporation and sputtering respectively.[11,12] Since theses deposition techniques require vacuum conditions, the layer fabrication is energy consumptive and difficult to apply on larger scales. Low cost methods like electroplating of stacked precursors with subsequent annealing resulted in efficiencies as high as 7.3%.[13] A different concept is the film fabrication through the deposition of synthesized CZTS NCs.[14] A device with 7.2% energy conversion efficiency using mechanically deposited CZTS-NCs and subsequent annealing in Se atmosphere has been demonstrated.[15] However, in this approach part of the NCs are lost during the deposition process. To use the NCs more economically, we developed a novel route to deposit the CZTS NCs.

[a]*Helmholtz-Zentrum Berlin für Materialien und Energie GmbH, Hahn-Meitner-Platz 1, D-14109 Berlin, Germany. E-mail: ennaoui@helmholtz-berlin.de*
[b]*Freie Universität Berlin, Berlin, Germany*

† Electronic supplementary information (ESI) available: See DOI: 10.1039/c3ra23093g

Electrophoretic deposition allows us to deposit all NCs onto the substrate without wasting the materials and allows the up-scaling of the deposited area. Moreover, the thickness of the resulting films can be easily controlled by tuning the concentration of the NCs solution.

## Experimental

### Materials

Zinc acetate dehydrate (98%) was purchased from Alfa-Aesar. Acetonitrile (anhydrous, 99.8%), toluene (ACS, $\geqslant$99.5%), oleylamine (technical grade, 70%), absolute alcohol, copper acetylacetonate (99.99%) and tin chloride dehydrate (>99.99%) were purchased from Sigma-Aldrich.

Molybdenum (Mo) coated soda lime glass substrates were prepared at the Helmholtz-Zentrum Berlin für Materialien und Energie (HZB) by sputter deposition. Fluorine doped tin oxide (FTO) substrates were acquired from Solaronix in form of (10 $\times$ 10) $cm^2$ plates.

### Synthesis of $Cu_2ZnSnS_4$ nanocrystals

CZTS NCs were synthesized by a one pot technique using oleylamine as both solvent and capping agent. The whole synthesis process was performed in air. In a typical synthesis, 2 mmol copper acetylacetonate, 1.5 mmol zinc acetate dihydrate, 1 mmol tin chloride, 4 mmol sulfur and 40 mL oleylamine were mixed in a three neck flask in air and then heated to 130 °C. After staying at this temperature for 30 min under magnetic stirring to allow the reaction precursors to dissolve in the solvent, the temperature was raised to 215 °C and kept at this temperature for 60 min. After cooling to room temperature, the NCs were isolated by precipitation with excess of ethanol and centrifugation. The precipitation and centrifugation process was repeated one more time. And the final NCs were dispersed in 10 mL toluene. The particles exhibit a sulfur poor/copper rich composition as determined by energy dispersive X-ray measurements (Cu: 28.2%, Zn: 13.4%, Sn: 13.0%, S: 45.4%).

### Dispersion preparation

A certain amount of highly concentrated CZTS NCs in toluene (mother dispersion) were diluted in a certain amount of toluene in a snap cap vial under the influence of a short (10 s–15 s) treatment with an ultra-sonic (US) tip. Before deposition the toluene–CZTS dispersion is mixed with a quantity of acetonitrile. Again, US-treatment is applied at equal conditions as before. Dispersion preparation was carried out in $N_2$ atmosphere.

### Electrophoretic deposition cell

We designed a cell to perform EPD on inch $\times$ inch or approx. (2.5 $\times$ 2.5 $cm^2$) sized substrates. The cell was manufactured at the HZB and consists of polytetrafluorethylene (Teflon). Substrates serve as counter (platinum) and working electrode (FTO, Mo) facing each other in a distance of 0.9 cm. When assembled a closed up volume for 1.76 mL of dispersion is formed. The deposited area has a size of 1.95 $cm^2$. Dispersion is added and recollected by a Pasteur pipette through one of two holes on the top side. Contacting is realized by two copper-rings placed around the dispersion cavity. The voltage is supplied by a power supply. The maximum current was set to 10 mA. The power supply was controlled by a LabView program.

### *In situ* monitoring setup

Quartz rods, inserted perpendicular to each other on two sides on the cell allow leading light through the colloidal dispersion during the deposition process. A set of light emitting diodes (LEDs) served as a light source and a Si-photodiode (Siemens BPW21) was used as a detector. During the deposition the detected light intensity changes as particles leave the dispersion to form a layer on the positive electrode. A pc-interface was used to process and display the detected signal strength in real time. The deposition experiments were performed inside a glove box under $N_2$ atmosphere.

### Characterization

Cross section scanning electron microscopy (SEM) images were taken of CZTS layers to determine their thickness and morphology. For analysis a Zeiss Leo Gemini 1530 with a thermal field emission cathode was used. The layers were examined by means of grazing incidence X-ray diffraction (GIXRD) using a Bruker AXS D8 Advance X-ray diffractometer. The radiation source was operated at a voltage of 40 kV and a current of 40 mA. The radiation of the Cu-K$\alpha$ (E = 8046 eV) was used for analysis. Measurements were performed in grazing incidence configuration with a step width of 0.02° and an integration time of 12.4 s per step. Reference X-ray diffraction patterns were taken from the powder diffraction database (PDF).

For Raman measurements a T64K Horiba system supplied with a solid-state Ti:Sa (titanium:sapphire) laser and a output power of 4 W was operated at a wavelength of 800 nm with an integration time of 10 min.

A Cary 500 UV-Vis-IR spectrometer was utilized for an optical characterization.

Light absorption measurements of CZTS NCs in dispersion before and after deposition were carried out with a double-beam spectrometer (PerkinElmer Lambda950 UV/Vis/IR) operating in the ultra-violet (UV) , visible (Vis) and infra-red (IR) regime.

## Results and discussion

### Electrophoretic deposition of $Cu_2ZnSnS_4$ nanocrystals

SEM images of the surface and cross section of CZTS NC layers on a Mo-substrate show densely packed layers Fig. 1. The

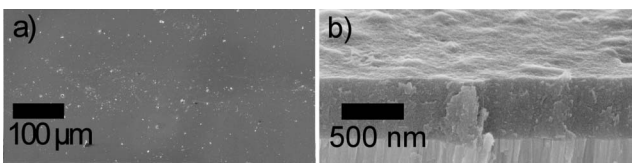


**Fig. 1** SEM image of a) the surface and b) the cross section of an electrophoretically deposited CZTS NC layer on a Mo-substrate.

 

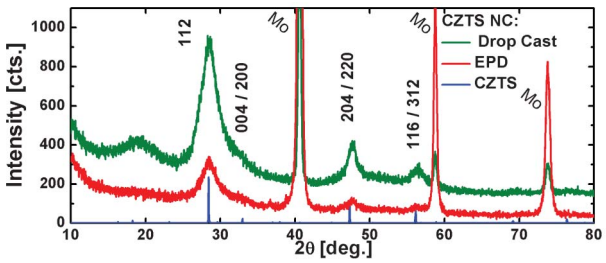


**Fig. 2** XRD reflexes of an electrophoretically deposited and a drop-casted CZTS NC layer on a Mo-substrate. No change in composition is detected. Differences in signal intensities are due to different layer thicknesses. CZTS reference spectra was taken from PDF.

layers exhibit a homogeneous surface without cavities at the layer/substrate interface.

GIXRD data of the deposited NC layers on MO-substrate exhibit strong signals at diffraction angles allocated to CZTS in literature ($2\theta$ = 28.53° (112), 47.33° (204)/(220), 56.16° (116)/(312)).[16] Signals at $2\theta$ = 40.52° 57.76°, 73.80° derive from the underlying Mo-substrate.[17] The diffractogram is shown in Fig. 2 together with data acquired from a drop-casted layer. Based on the GIXRD analysis CZTS is identified as the dominant phase present in the layers. The difference in signal intensity is allocated to a larger layer thickness of the drop-casted sample. This is assured by the considerably weaker Mo-signal in the respective diffractogram. The XRD analysis does not show a chemical change imposed by the EPD process on the NCs.

Fig. 3 shows a vibrational spectra of the CZTS NC layer obtained from Raman analysis. The data is fitted with superposition of five Lorentz curves. The peaks at R1: 255 $cm^{-1}$, R3: 335 $cm^{-1}$, R4: 357 $cm^{-1}$, R5: 373 $cm^{-1}$ coincide with the characteristic vibrational modes assigned to CZTS in literature,[18,19] with R3 as the CZTS A-mode. The discrepancy between the peak position of R2 (300 $cm^{-1}$) and the CZTS vibrational mode usually detected at 287 $cm^{-1}$ could be an

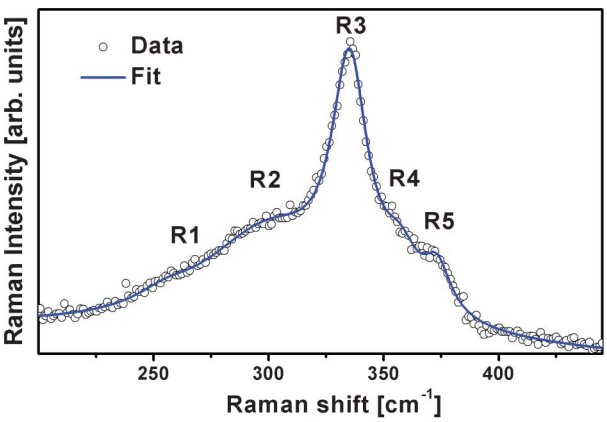


**Fig. 3** Raman spectra of an electrophoretically deposited CZTS NC layer on a Mo-substrate. The spectra features the vibrational modes assigned to CZTS in literature. No secondary phases of CZTS are detected.

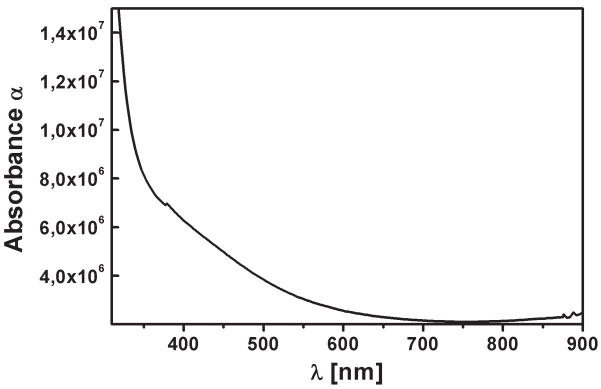


**Fig. 4** Dependence of the wavelength $\lambda$ on the absorbance $\alpha$ of a CZTS NC layer on FTO determined by UV-vis measurements.

indication of impurity phases present. Considering the copper rich/sulfur poor particle composition the peak could be an indication of cubic $Cu_2SnS_3$ with the strongest vibrational modes at 303 $cm^{-1}$ and 355 $cm^{-1}$.[20]

However, since the peaks are not discrete an unambiguous interpretation is not possible.

Absorbance of the electrophoretically deposited CZTS NC layers was analysed by UV-vis measurements. Fig. 4 shows the absorbance of a CZTS NC layer of approx. 500 nm on an FTO coated glass substrate. With an absorbance around the visible range $10^6$ $cm^{-1}$ the value is higher than others reported in literature (see above). This discrepancy can be explained by internal reflection at the interfaces of the soda lime glass/FTO/CZTS multilayer system and addition absorption of the substrate material itself. As it can be seen in Fig. 4 the influence of the glass substrate becomes dominant in the UV region (350 nm).

In a series of experiments the relative concentration of NCs in dispersion was varied. The resulting layer thickness was determined by the analysis of SEM cross section images. The thickness of the layers increased with increasing concentration of CZTS NC dispersions. The relationship between the thickness of the CZTS NC layers and the relative concentration of the dispersions is shown in Fig. 5. As it can be seen, the thicknesses of the layers varied from 200 nm to 1.4 μm when

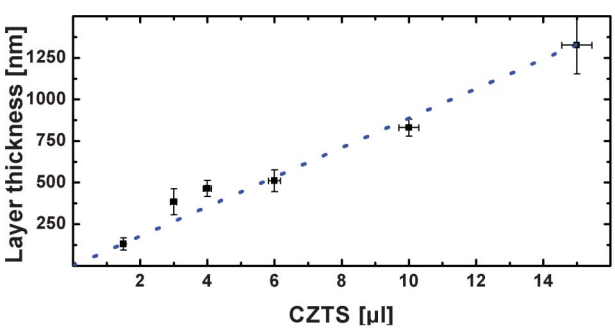


**Fig. 5** Layer thickness as determined by SEM cross sectional images and the amount of CZTS mother dispersion. A linear correlation is observed.

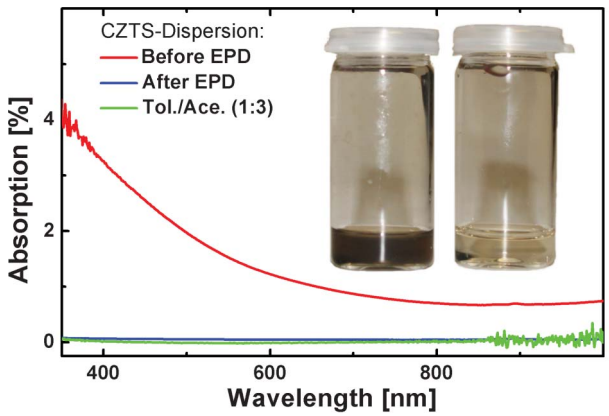


**Fig. 6** UV-Vis-IR absorption spectra of dispersions before (red), after (blue) the deposition process and a pure mix of solvents as reference (green). Complete depletion of CZTS NCs is achieved during deposition.

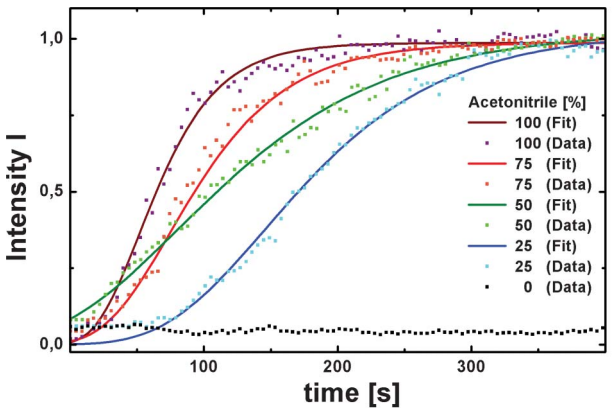


**Fig. 7** Transmission curves measured with a step size of 0.3 s during EPD of with dispersions of different acetonitrile contents. Deposition velocity rises with the acetonitrile content. Without the addition of acetonitrile, no deposition is observed. In the experiments a voltage of 100 V was applied.

the amount of the mother solution changed from 1.5 μL to 15 μL. Interestingly, we found that the thickness of the layers show a linear dependence on the relative concentration of the CZTS NCs.

Layers obtained from dispersions below 1.5 μL lacked of complete substrate coverage. Uneven distribution of particles could be caused by spatial inhomogeneities of the electric field. Layers with a thickness above 1.4 μm exposed an increasing amount of cracks. These cracks may be the result of growing tensions due to evaporation of residual solvent.

The linear relationship is connected to the complete NC depletion of the dispersion during the deposition. Fig. 6 shows UV-vis-IR spectra of the dispersion (3 : 1 acetonitrile and toluene) before and after the appliance of a potential of 100 V for 5 min. The residual solvent shows similar characteristics as a mix without added NCs. The inset shows photographs of the respective dispersion before and after the deposition.

### *In situ* monitoring

The prior results qualify the light absorption as an indicator for the progress of the deposition process. By measuring its relative change during the EPD beginning and end as well as the dynamics of the deposition can be determined.

The data obtained from the *in situ* transmission measurements was fitted by the formula

$$I = I_0 \exp\left(-C \cdot \exp\left(-k\left(t - t_i\right)\right)\right) \quad (1)$$

where the absorption parameter $C$ is defined as $C = \alpha\, x\, c_0$ with the absorption coefficient $\alpha$, the initial NC concentration $c_0$ and the distance between passed in the solution by the light $x$. The values of $C$ depend on the initial conditions $C = -ln(I(0))$. The variable $k$ denotes the kinetic factor defined as $k = \mu\, E\, S\, v^{-1}$ where $\mu$ is the electrophoretic mobility, $E$ the applied electric field, $S$ the electrode area and $v$ the cavity volume. In order to imply the possibility of retardation, the variable $t_i$ was introduced. Details about the derivation can be found in the ESI.†

In a first experiment the acetonitrile/toluene ratio was varied while leaving the NC concentration and the applied voltage constant.

To study the influence of the acetonitrile and toluene on the deposition process we performed a series of experiments where the acetonitrile/toluene ratio was varied while keeping the other conditions constant.

Depositions using dispersions with varying acetonitrile content (0%, 25%, 50%, 75% and 100%) and 5 μL of CZTS mother dispersion were exerted with a voltage of 100 V in 20 min. The data recorded during the depositions is presented in Fig. 7.

The curves show an increasing transmission value over time, indicating the migration of particles to the electrode. Dispersions with an acetonitrile/toluene ratio greater than zero lead to the deposition of a NC film, whereas the dispersion without acetonitrile did not lead to a deposition. The transmission value remains at a constant level, indicating no change in NC concentration in dispersion. The kinetic parameter $k$ and the retardation time $t_i$ used for fitting the data are shown in Fig. 8. Higher acetonitrile content leads to a higher value of $k$. As the area $S$ and the Volume $V$ are constant, an increasing value of $k$ implies an increasing electrophoretic mobility $\mu$. A general expression for the electrophoretic mobility is given by the Henry equation:

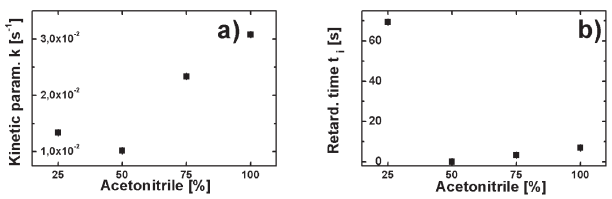


**Fig. 8** a) Kinetic parameter $k$ and b) retardation $t_i$ in dependence of the acetonitrile ratio in the CZTS NC dispersion.

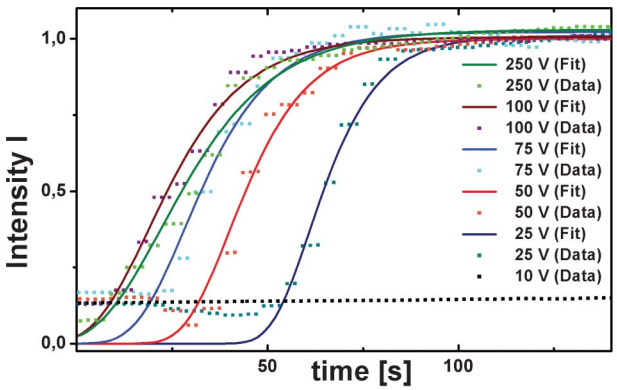


**Fig. 9** Transmission curves acquired with a step size of 0.8 s during the deposition processes at potentials of 10 V, 25 V, 50 V, 75 V, 100 V and 250 V. The acetonitrile toluene ratio was 3 : 1 for all dispersions. With decreasing voltage an increasing retardation $t_i$ is observed.

$$\mu = \frac{\psi \cdot \varepsilon_r \varepsilon_0}{\eta} f(k,r) \quad (2)$$

where $\psi$ denotes the zeta potential, $\varepsilon_0$ dielectric constant, $\eta$ the viscosity of the solvent and $\varepsilon_r$ its permittivity.

The permittivity and the viscosity of a dispersion have a direct influence on the electrophoretic mobility of the dispersed particles.

A lower viscosity and a higher permittivity lead to a higher electrophoretic mobility. By addition of acetonitrile to toluene the permittivity increases, while the viscosity decreases.[21] This leads to a higher value of $\mu$. If acetonitrile causes the particles surface charge, a higher amount of acetonitrile could also lead to increasing charge on the particles and a higher zeta potential. The experiments suggest that the electrophoretic mobility of dispersed particles can be tuned by the ratio of acetonitrile in dispersion.

To examine the effect of the applied voltage on the deposition process we conducted another series of experiments by using different voltages, 10 V, 25, 50 V, 75 V, 100 V and 250 V. The acetonitrile/toluene ratio was kept constant at 3 : 1, the amount of CZTS NC mother dispersion at 5 μL and the deposition time was set to 20 min. FTO was used as substrate.

The recorded curves are shown in Fig. 9 together with their respective fits. The curves acquired during the EPD processes show an increasing retardation time $t_i$ and a slight increase in the kinetic parameter $k$ with decreasing voltage. The values are illustrated in Fig. 10. Note that at a voltage of 10 V the curve remains at a constant value, indicating that no deposition takes place. The findings suggest the existence of a threshold voltage.

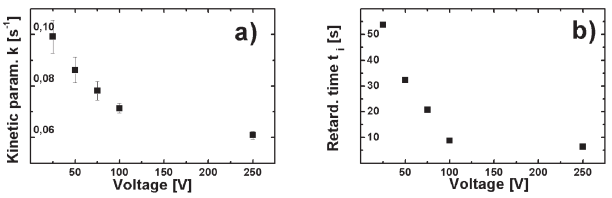


**Fig. 10** The kinetic parameter $k$, and the retardation time $t_i$ are shown deriving from transmission curves of voltage dependant measurements.

The obtained results concerning the deposition process oppose the theory of charge generation due to the polarity of adsorbed surfactants. As all dispersions were prepared under the same conditions the same particle charge would be expected.

This would lead to an increased acceleration with increasing voltage, in contrast to our experiments. Additionally, the particles would carry a charge directly after the addition of acetonitrile. However, in the experiments a delay between the appliance of a potential and initiation of the particle migration was observed. The delay increased with decreasing voltage. The velocity of deposition increased, as indicated by an increasing kinetic parameter $k$. These interpretations of the measurements suggest that the applied voltage has an influence on charge generation. This requires further investigation.

Using the transmission setup the deposition progress over time could be evaluated. It was found that the deposition process is completed in a time range of 30–90 s depending on the applied voltage and acetonitrile/toluene ratio (Fig. 7, Fig. 9).

## Conclusions

CZTS NC films were deposited on FTO and Mo-coated glass substrates by an electrophoresis deposition method. The deposited films are homogeneous, compact and form a closed interface with the substrate material. XRD and Raman analysis confirmed CZTS to be the major phase present in the films. The dispersion based on toluene and acetonitrile depleted entirely during the deposition process. The layer thickness was controllable *via* the concentration of CZTS NC in dispersion, showing a linear correlation.

A setup was developed to directly monitor the deposition process by the decrease of the relative particle concentration over the time. This allowed a first insight into particle behavior during the deposition process and enabled the determination of the deposition duration.

Due to the fast deposition times (30–90 s), low energy deposition process and the economic material use, electrophoretic deposition constitutes a new potential low cost route for the fabrication of CZTS solar cell absorber layers.

## Acknowledgements

This work was carried out as part of a program supported by the BMBF (Grant 03SF0363B). The authors would like to thank Ulrike Bloeck for the TEM and EDX measurements and Patryk Kusch for assistance with the Raman analysis. One of the authors (Xianzhong Lin) gratefully acknowledges the financial

support from the Chinese Scholarship Council, HZB and Helmholtz Association.

## References

1 P. Sarkar and P. S. Nicholson, *J. Am. Ceram. Soc.*, 1996, **79**, 1987–2002.
2 O. O. Van der Biest and L. J. Vandeperre, *Annu. Rev. Mater. Sci.*, 1999, **29**, 327–352.
3 *Electrophoretic Deposition of Nanomaterials*, ed. J. H. Dickerson and A. R. Boccaccini, Springer, 2012.
4 S. Ahmed and K. M. Ryan, *Chem. Commun.*, 2009, 6421–6423.
5 J. Li and I. Zhitomirsky, *J. Mater. Process. Technol.*, 2009, **209**, 3452–3459.
6 S. J. Limmer and G. Cao, *Adv. Mater.*, 2003, **15**, 427–431.
7 H. Katagiri, *Thin Solid Films*, 2005, **480–481**, 426–432.
8 K. Ito and T. Nakazawa, *Jpn. J. Appl. Phys.*, 1988, **27**, 2094–2097.
9 T. Unold and H. W. Schock, *Annu. Rev. Mater. Res.*, 2011, **41**, 297–321.
10 T. K. Todorov, J. Tang, S. Bag, O. Gunawan, T. Gokmen, Y. Zhu and D. B. Mitzi, *Adv. Energy Mater.*, 2013, DOI: 10.1002/aenm.201200348.
11 B. Shin, O. Gunawan, Y. Zhu, N. A. Bojarczuk, J. S. Chey and S. Guha, *Prog. Photovolt. Res. Appl.*, 2011, 1174.
12 H. Katagiri, K. Jimbo, S. Yamada, T. Kamimura, W. S. Maw, T. Fukano, T. Ito and T. Motohiro, *Appl. Phys. Express*, 2008, **1**, 041201.
13 S. Ahmed, K. B. Reuter, O. Gunawan, L. Guo, L. T. Romankiw and H. Deligianni, *Adv. Energy Mater.*, 2012, **2**, 253–259.
14 C. Steinhagen, M. G. Panthani, V. Akhavan, B. Goodfellow, B. Koo and B. A. Korgel, *J. Am. Chem. Soc.*, 2009, **131**, 12554–5.
15 Q. Guo, G. M. Ford, W. C. Yang, B. C. Walker, E. A. Stach, H. W. Hillhouse and R. Agrawal, *J. Am. Chem. Soc.*, 2010, **132**, 17384–17386.
16 (PDF #00-026-0575).
17 (PDF # 00-042-1120).
18 P. A. Fernandes, P. M. P. Salome and A. F. da Cunha, *J. Alloys Compd.*, 2011, **509**, 7600–7606.
19 F. Jiang, H. Shen, W. Wang and L. Zhang, *Appl. Phys. Express*, 2011, **4**, 074101–3.
20 P. A. Fernandes, P. M. P. Salome and A. F. da Cunha, *Thin Solid Films*, 2009, **517**, 2519–2523.
21 G. Ritzoulis, N. Papadopoulios and D. Jannakoudakis, *J. Chem. Eng. Data*, 1986, **31**, 146–148.



 